International Journal of Mass Spectrometry and Ion Processes, 106 (1991) 79–115
Elsevier Science Publishers B.V., Amsterdam

OPERATION OF A QUADRUPOLE ION TRAP MASS SPECTROMETER TO ACHIEVE HIGH MASS/CHARGE RATIOS

RAYMOND E. KAISER, Jr. and R. GRAHAM COOKS
Department of Chemistry, Purdue University, West Lafayette, IN 47907 (U.S.A.)

GEORGE C. STAFFORD, Jr. and JOHN E.P. SYKA
Finnigan MAT, 355 River Oaks Parkway, San Jose, CA 95134 (U.S.A.)

PHILIP H. HEMBERGER
Los Alamos National Laboratory, Los Alamos, NM 87545 (U.S.A.)
(Received 20 July 1990)

ABSTRACT

One of the principal limitations of the commercial quadrupole ion trap mass spectrometer is the relatively low limiting value of mass/charge ratio (650 Da per charge). This constraint limits applications of desorption ionization techniques which can produce ions of many thousand Da per charge. Several techniques for extending the mass/charge range of the quadrupole ion trap are presented. These include (i) the use of smaller electrodes, (ii) operation at lower radio frequencies, and (iii) resonance ion ejection using a voltage of appropriate frequency, applied symmetrically across the end-cap electrodes during the mass scan. The performance of each of these methods is compared using external ionization of alkali halide salts with Cs^+ bombardment. Special attention is given to the effects of scan rate on resolution and a method of reducing the scan rate without loss of data is described. Mass measurement accuracy is studied in some detail, the mass shifts which occur using resonance ejection are characterized and this information is used to correct mass assignments.

The relative merits of the three methods of mass range extension are assessed. Field inhomogeneities in the particular smaller electrodes used here apparently cause some loss of performance in these devices making them the least successful of the methods. Frequency reduction gives excellent results over a limited range of m/z values. However, resonance ejection can be used alone to achieve an even greater m/z extension and is the (single) method of choice. A combination of modest size and frequency reduction with axial modulation is probably an ideal solution for high mass biological mass spectrometry. Performance at high mass is illustrated by recording data on CsI clusters and on peptides. These experiments show that mass/charge measurements are accurate to better than 0.1% without external calibration, that a mass resolution of 3000 FWHM is achieved (unit resolution at 50% valley to 3000), and that a mass/charge range in excess of 70 000 Da per charge is accessible.

0168-1176/91/$03.50

INTRODUCTION

Ions are normally generated within the cavity of the ion trap using electron impact, positive chemical ionization [1] or negative chemical ionization [2]. Recently, methods have been reported for trapping ions generated in external ion sources [3,4]. Modern ionization methods such as secondary ion mass spectrometry (SIMS) [5] and laser desorption (LD) [3], as well as electrospray [6], have been implemented with an ion trap allowing the generation of ions from involatile samples. To exploit these new ionization capabilities, and the ability for efficient dissociation of trapped ions in the course of tandem MS experiments using a supplementary frequency to excite (but not eject) trapped ions [7], the mass range of the ion trap must be extended beyond the 650 Da per charge limit of the commercial system. Previously, we have communicated briefly on two methods for extending the mass range of the ion trap, reduction in the trapping volume [8] and the use of axial modulation [5]. This report presents details of these methods and the frequency reduction procedure. It also compares the performance of each of these techniques for extending the mass range of the quadrupole ion trap.

Operating modes

In recent years, the quadrupole ion trap mass spectrometer, operated in the mass-selective instability mode [9], has become increasingly important in chemical analysis [10–12]. In this method, an r.f. voltage is applied to the ring electrode, while the two end-cap electrodes are held at ground potential. All ions whose m/z ratios exceed a minimum cut-off value (which occurs at a fixed value of q_z and is therefore linearly dependent upon the amplitude of the r.f. voltage) are trapped. To record a mass spectrum, the r.f. voltage is increased with time so that ions of successively greater m/z ratios develop unstable trajectories, are ejected through perforations in an end cap, and are detected at an external electron multiplier. Before the introduction of the mass-selective instability scan mode, the ion trap was used primarily as a reactor for gas phase ion/molecule reactions with mass analysis of the products being accomplished by transferring the ions to a conventional quadrupole analyzer [13].

The theory of ion motion within conventional quadrupole mass filters and quadrupole ion traps was presented by Paul and co-workers [14,15] in their early papers describing the devices. From the well known solutions to the Mathieu equations, it is possible to generate a parameterized stability diagram [9], characterizing the solutions to the equations of motion for an ion in the applied three-dimensional quadrupole field. The most important characteristic of the trajectory of an ion is whether it is stable or unstable; if the a_z, q_z Mathieu parameters fall within the shaded region indicated in Fig. 1, the

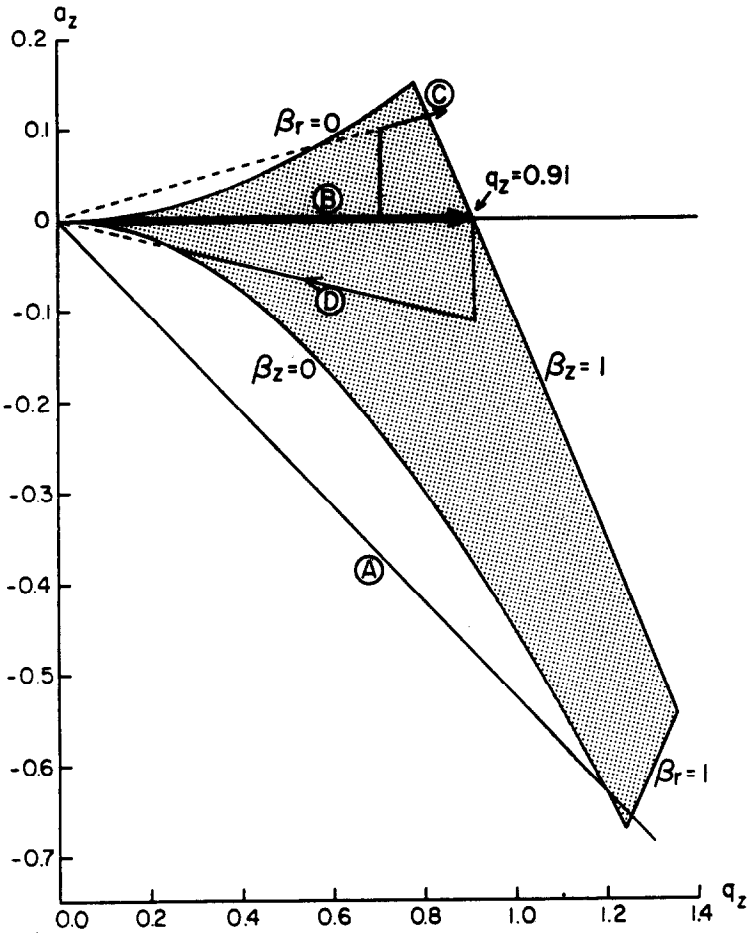

Fig. 1. Mathieu stability diagram illustrating different modes of scanning the ion trap. (A) Mass-selective stability scan line. (B) Mass-selective instability scan line. (C) Forward r.f./d.c. scan line for mass range extension relative to scan line B. (D) Reverse r.f./d.c. scan line for mass range extension relative to scan line B.

trajectory can be stable, provided the initial velocity and position of the ion is not such that it strikes an electrode. Outside the area indicated, the trajectory is unstable regardless of the initial velocity and position. An ion must have a stable trajectory in both the r (radial) and z (axial) directions and motion in these directions is separable.

The parameterized coordinates (coefficients in the Mathieu equation) of the stability diagram are:

$$q_z = 4eV/mr_0^2\Omega^2 \tag{1}$$

and

$$a_z = -8eU/mr_0^2\Omega^2 \quad (2)$$

where V is the r.f. peak voltage level, U is the d.c. voltage applied to the ring electrode, r_0 is the inscribed radius of the ring electrode, Ω is the angular frequency of the r.f. voltage, m is the mass of the ion, and e is its charge. A less common, more general representation of the Mathieu equation coefficients defines q_z and a_z in terms of both z_0 (the distance from the center of the trapping cavity to the apex of the end-cap electrode) and r_0 [16]:

$$q_z = 8eV/m(r_0^2 + 2z_0^2)\Omega^2 \quad (3)$$

and

$$a_z = -16eU/m(r_0^2 + 2z_0^2)\Omega^2 \quad (4)$$

Eqs. (3) and (4) are not bound by the restraints implicit in deriving Eqs. (1) and (2) that $r_0 = 2^{1/2}(z_0)$.

In Fig. 1, the operating line for the mass-selective instability mode (scan line B) is compared with several other operating modes. If the scan line A is used (mass-selective stability) ions covering a narrow range of masses are stable and to assemble a mass spectrum one must perform a separate experiment for each m/z value. Because of this, a common option before the introduction of the mass-selective instability scan mode was simply to use the ion trap as an ion reaction chamber and to employ an external analyzer for mass analysis.

In the mass-selective instability mode (scan line B in Fig. 1), operating along the q_z axis of the stability diagram, the maximum value of q_z is 0.908. At this point ions become unstable axially and leave the ion trap through the apertures in the end-cap electrodes. Since the r.f. voltage is scanned to sequentially eject ions of increasing m/z ratios, the upper mass limit of the system is ultimately determined by the maximum amplitude of the r.f. voltage (V_{max}). Thus, through manipulation of Eq. (3), the upper mass limit, $(m/z)_{max}$, of an ion trap operated in the mass-selective instability mode is given as:

$$(m/z)_{max} = 8V_{max}/q_{eject}(r_0^2 + 2z_0^2)\Omega^2 \quad (5)$$

where q_{eject} is the point on the stability diagram where the ion becomes unstable and is ejected (which under normal operating conditions is $q_{eject} = 0.908$). The commercial Finnigan ion trap has a nominal operating mass/charge limit of 650 Da per charge; if one calculates the actual mass limit from the operating parameters as given in Table 1, the calculated mass limit is 663 Da per charge. Scans C and D are discussed below.

Mass range extension

From inspection of Eq. (5), it is possible to increase the mass/charge range of the ion trap in four ways: (i) by reducing the trapping dimensions, (ii) by

TABLE 1

Normal operating parameters for the ion trap

Radio frequency ($\Omega/2\pi$)	1.1 MHz
Radius of ring electrode (r_0)	1.0 cm
Distance from center to end-cap electrode (z_0)	0.707 cm
r.f. maximum voltage	15 000 V_{p-p}
q_{eject}	0.908
Maximum detectable m/z for these parameters	663 Da

increasing the maximum r.f. voltage, (iii) by decreasing the r.f. frequency applied to the ring electrode, and (iv) by selecting a point on the stability diagram other than the normal q_{eject} value of 0.908 to cross from stability to instability. Note that all the experiments described in this paper extend the mass-to-charge range; extension of mass range by increasing the charge is not a topic of the paper and when not specified a charge state of unity is implied.

Previously, only a few attempts had been made to increase the mass limit of the ion trap beyond the 650 Da per charge restraint. Stafford and Syka [17] successfully increased the mass limit by using method (i), changing the trap dimensions such that $r_0 = 7$ mm and $r_0 = z_0$. In this configuration, a mass limit of approximately 850 Da was achieved, yielding a mass/charge increase of a factor of 1.3 × compared with that of the commercial system.

We are unaware of attempts to increase the mass/charge range by the second method, increasing the r.f. voltage. The third method, decreasing the r.f. frequency, is discussed below. The final method (iv) for mass range extension was reported by Todd et al. [18] who introduced the concept of moving off the $a_z = 0$ line of the stability diagram during the mass analysis scan. This results in ejecting ions at a lower q_{eject} value than the normal instability limit of $q_{eject} = 0.908$. Scan line C in Fig. 1 illustrates this case, a negative d.c. potential of appropriate magnitude being applied to the ring electrode during the mass analysis scan. This procedure moves the working point for a given ion from the q_z axis into the upper region of the stability diagram. When the d.c. potential is maintained at a constant fraction of the r.f. amplitude, that is, at a constant d.c./r.f. ratio, voltage scans allow mass-selective instability to be achieved near the apex of the stability diagram. In this case, ions become unstable at $q_{eject} = 0.814$, and according to Eq. (5), the mass range of the ion trap is extended modestly to 725 Da (1.12 × increase) by this procedure.

From inspection of Fig. 1, the lower portion of the stability diagram can also be used to change the mass/charge range in a similar fashion to that described above. If one applies a positive d.c. potential to the ring electrode

during the normal mass-selective instability r.f. scan, ions would still be ejected from the trap at the $\beta_z = 1$ instability line but at higher q_{eject} values than normal, thereby lowering the mass range. However, if ions were ejected from the trap at the $\beta_z = 0$ instability line, much lower q_{eject} values would be achieved as shown by scan line D in Fig. 1. This requires scanning the r.f. voltage in what Todd et al. [18] have termed a "reverse-scan", the d.c. and r.f. amplitudes being ramped downwards while maintaining a constant r.f./d.c. ratio. For example, by ejecting ions from the $\beta_z = 0$ line at $q_{eject} = 0.27$, a theoretical mass limit of 2185 Da (3.4× increase) is possible. Using this method, ions of m/z 1466 derived from tris(perfluorononyl)-*s*-triazine have been ejected mass-selectively from the ion trap and detected externally. Nothing is known of the resolution which can be achieved using reverse scans, nor to what extent the value of q_{eject} can be decreased without loss in performance. However, the fact that the scan line approaches the stability boundary at an oblique angle is expected to limit the resolution obtainable.

EXPERIMENTAL

Reduction in trapping dimensions

A quadrupole ion trap electrode structure having half the dimensions of those in the commercial Finnigan ion trap instrument, was built and initially characterized in a Finnigan ion trap detector (ITD) using volatile fluorinated compounds which could be studied via electron ionization (EI) [8]. Because of the success achieved using these half-sized electrodes, two other sets were later machined having a third and a fourth the dimensions of the commercial electrodes. The one-third and one-fourth sized electrodes could not be adequately characterized using the limited mass/charge range available via EI, but desorption ionization methods, together with procedures for ion injection, allowed their characterization as described below.

The electrode design used for the high mass electrodes conforms to theoretical calculations for the surfaces and for the spacings between the electrodes [14]. The end-cap electrodes have surfaces corresponding to hyperboloids of two sheets:

$$r^2 - 2z^2 = r_0^2 \tag{6}$$

Where r and z are radial and axial coordinates, and r_0 is the radius of the ring electrode. The ring electrode has a surface corresponding to a hyperboloid of one sheet:

$$r^2 - 2z^2 = -r_0^2 \tag{7}$$

The spacing between the end caps and the ring electrode followed the equation:

$$r_0^2 = 2z_0^2 \tag{8}$$

where z_0 represents the distance from the center of the trapping area to the vertex of the end-cap electrode.

The new electrodes were machined to tolerances of 0.0001 in. to calculated surface profiles using numerically controlled machine tools in the Los Alamos shops. The material used was 304 stainless steel. Instead of having to machine new mountings, only the hyperbolic surfaces were redesigned and machined. The electrodes were designed to be directly interchangeable with the Finnigan electrodes so that standard electronics and software could be used to evaluate their performance at high mass. The half-, third- and quarter-sized electrode inserts were machined such that $r_0 = 5\,\text{mm}$, $r_0 = 3.3\,\text{mm}$ and $r_0 = 2.5\,\text{mm}$, respectively. Eqs. (6) through (8) were used to produce the correct hyperbolic contours on the electrodes. Spacing of the electrodes was accomplished using ceramic insulators. A series of seven small holes (1/16 in. diameter) were drilled through the vertex of the exit end-cap electrode in the one-half sized electrodes and a single hole (1/16 in. diameter) was drilled into the one-third and one-quarter sized electrodes to allow unstable ions to pass from the ion trap into the electron multiplier. All entrance electrodes employed a single 1/16 in. diameter aperture.

Two sets of small electrodes, those of half- and quarter-size, were characterized in this study using Cs^+ SIMS [5]. The half-sized ion trap, Cs^+ ion gun and ion injection assembly are shown in cross-section in Fig. 2. The ion trap

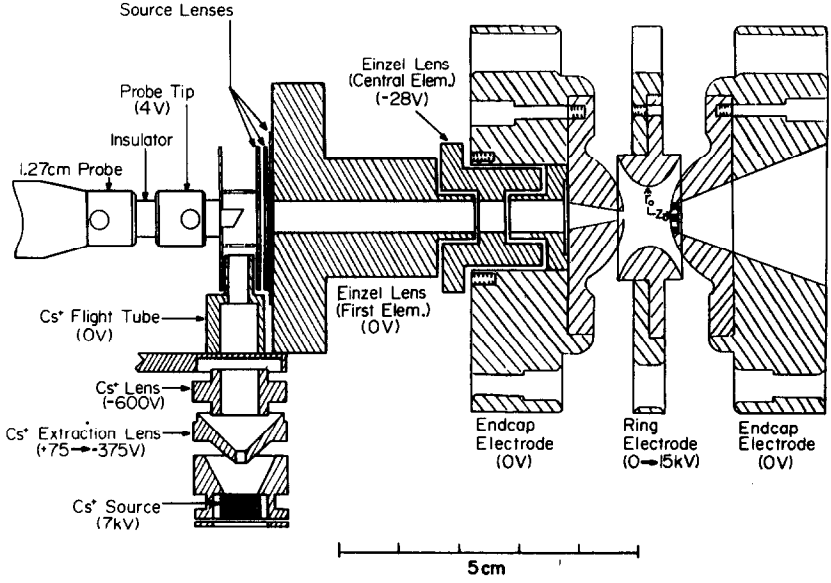

Fig. 2. Cross-sectional view of the instrumental configuration for Cs^+ desorption ionization and ion injection into a reduced-sized quadrupole ion trap mass spectrometer.

mass spectrometer (ITMS) used in this study has been described previously [7]. The ion source and injection system is described below.

Reduction of the r.f. drive frequency

There are instrumental factors which arise that affect the mass limit and mass scale of an ion trap instrument when the r.f. drive frequency is changed. The r.f. amplitude control system relies on a capacitor divider scheme to feed back the r.f. voltage being applied to the ring electrode. The impedance of the detector capacitor, X_C, determines the proportionality between the output by the r.f. control DAC and the actual r.f. voltage applied to the trap ring electrode. Since, as shown in Eq. (9) where f is the frequency and C is the capacitance, the impedance of a capacitor varies inversely with frequency, the proportionality between the output of the r.f. control DAC and the amplitude of the r.f. voltage applied to the ring electrode also varies inversely with r.f. frequency.

$$X_C = 1/(2\pi fC) \tag{9}$$

Therefore, when lowering the r.f. drive frequency, the combination of the effects described by Eqs. (5) and (9) yields a proportionality between the r.f. DAC output and the m/z at any particular q_{eject} that varies as $(1/f)^3$. The instrument data system assigns masses based on the standard operating r.f. frequency, f_{std}, of 1.1 MHz, a standard q for ejection, $q_{\text{eject-std}}$, of ca. 0.908 and a standard upper m/z limit at full r.f. DAC output of 650 Da per unit charge. A data system assigned mass-to-charge ratio, m/z_{std}, converts to a true mass-to-charge ratio, m/z_{new}, according to the relationship in Eq. (10).

$$(m/z)_{\text{new}} = (m/z)_{\text{std}} \cdot (q_{\text{eject-std}}/q_{\text{eject-new}}) \cdot (f_{\text{std}}/f_{\text{new}})^3 \tag{10}$$

The quantities $q_{\text{eject-new}}$ and f_{new} are the ejection q and the r.f. frequency of the modified ion trap system.

Provided that the r.f. generation electronics has sufficient reserve voltage generation capability so that the amplitude of the r.f. voltage applied to the trap ring electrode tracks the r.f. DAC output over its full 0–10 V range, the mass limit of an ion trap operated at a reduced r.f. frequency can be expressed by Eq. (10) if m/z_{std} is assigned the value of the standard upper m/z limit of the commercial trap, 650 Da per unit charge. How the maximum attainable amplitude of the r.f. voltage that the r.f. generation electronics can produce varies with operating frequency depends upon the band pass characteristics of the r.f. power amplifier/generator and the efficiency of the resonant r.f. transformer.

Two different sets of experiments were performed at frequencies lower than 1.1 MHz. The first set of experiments modestly reduced the r.f. drive fre-

quency to 0.921 MHz resulting in a mass limit of 1105 Da per unit charge (1.7 × increase) as can be calculated from Eq. (10). The r.f. power amplifier/generator required only the minor modification of having its standard crystal replaced with one appropriate for generating a 0.921 MHz waveform. However, this frequency change required substantial modification of the tuned r.f. transformer. The r.f. transformer is essentially an LC tuned circuit. The resonant frequency of a tuned circuit is given as:

$$f = (LC)^{-1/2} \tag{11}$$

where in this case L is the inductance of the air core coil and C is a lumped tuning capacitance that includes the capacitance between the ion trap ring electrode and the end caps, the capacitance of any capacitors placed between the transformer coil's secondary tap and ground, and the stray capacitance of the coil assembly. While from Eq. (11) it can be seen that adding either capacitance or inductance to the resonant transformer will reduce its resonant frequency, it is well known that the most efficient conversion of r.f. power to r.f. volts is accomplished when the capacitance is minimized. The commercial transformer coil was therefore replaced with a transformer coil having substantially higher inductance. This special coil consists of a smaller diameter coil mounted inside and connected in series with a standard coil. This transformer coil could be tuned to 0.921 MHz using only the trap electrode and stray capacitances as the tuning capacitance. By minimizing the tuning capacitance at 0.921 MHz this special transformer assembly allowed more efficient conversion of r.f. power available from the r.f. amplifier/generator electronics thus yielding the 1.7 times increase in mass range.

In the second set of frequency reduction experiments, a more significant frequency reduction, to 0.6 MHz, was accomplished. These experiments required further modification to the r.f. transformer as well as significant modifications to the r.f. power amplifier/generator beyond a simple crystal change. Extra capacitance (ca. 30 pf) had to be added to the r.f. resonant transformer in order to attain a resonant frequency of 0.6 MHz. Within the r.f. power amplifier/generator various component values were changed as well as the ferrite core material used for transformers and inductors in order to obtain a reasonable r.f. power output at this low frequency. These modifications allowed the instrument to attain a m/z range of 2275 Da per unit charge. At this frequency the r.f. amplitude was only able to track the r.f. DAC output over 57% of its range which corresponds to a maximum r.f. voltage similar to that accessible at the standard operating frequency.

Operation of the ion trap at 0.921 MHz and 0.6 MHz was characterized using Cs^+ SIMS. CsI and RbI were used as the samples. The secondary ion injection energy was constant at approximately 4 eV (the ion volume was held at 4 V above ground) and the helium pressure was maintained at 1.2 mTorr.

Resonance ejection

A supplementary a.c. voltage may be applied between the end-cap electrodes of the ITMS in order to excite trapped ions and hence cause collision activated dissociation and so allow MS–MS experiments [3]. In the experiments described in this section, a supplementary a.c. voltage of 15 V_{p-p} and of selected fixed frequency, chosen to be in the range of 4 kHz to 550 kHz, was applied during the mass-analysis scan. As an ion of a particular m/z ratio acquires the frequency of the applied supplementary a.c., it acquires kinetic energy and is resonantly ejected from the ion trap. Figure 3 shows the scan program used.

To improve resolution using axial modulation a "key sequence" program was written to increment the modulation voltage in 100 mV steps. An external r.f. amplifier (controlled by using the 0–10 V DAC output which normally regulates the supplementary a.c. voltage amplitude) was used in order to supply a maximum of 40 V_{p-p}; whereas, the r.f. supply system was only able to supply a maximum of approximately 12 V_{p-p}. The offset DAC method (see Results and Discussion) was used to insure that the experiment would not be limited by the resolution of the data collection rate at higher masses and to observe mass shifts with better accuracy. The r.f. voltage applied to the ring electrode during ion injection was optimized for the observed mass range. Cs^+ SIMS ionization of CsI generated cluster ions covering the entire mass/charge range of interest was used for these experiments.

Desorption ionization

Desorption ionization was accomplished externally to the ion trap and was followed by injection of the secondary ions [3,5]. The cesium ion gun (Antek,

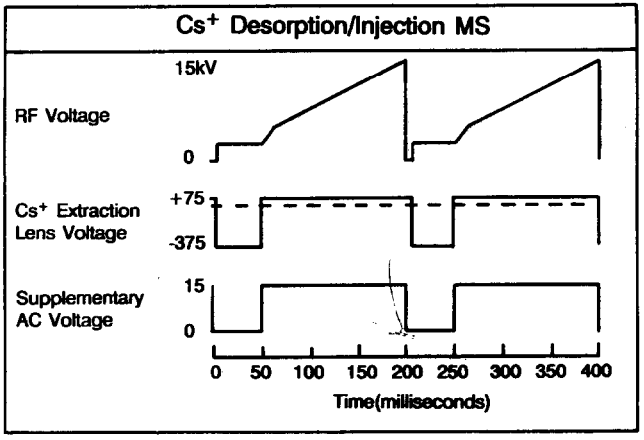

Fig. 3. Ion trap scan program used to record mass spectra generated by Cs^+ SIMS as illustrated in Fig. 2.

Palo Alto, CA) [19] used in this study was modified in order to facilitate mounting and to shield the cesium beam from the ceramic insulators of the source. The Cs^+ source, extraction lens and focussing lens were mounted to a ceramic block which was secured to a mounting bracket. The Cs^+ exit lens and the Cs^+ flight tube were custom-fabricated from stainless steel and employed to direct the Cs^+ beam towards the sample. An external power supply allowed variable potentials to be applied to the source, and to the extraction and focussing lenses. The mounting bracket, exit lens and flight tube were all held at ground potential.

The primary Cs^+ beam was focussed onto the ceramic insulated stainless steel probe tip (45° angle, area of probe tip 5.4 mm^2) with the probe positioned in an ion volume. The ion volume, which was taken from a Finnigan 3200 electron ionization source, establishes the potential at which the probe was held, thereby giving the secondary ions a kinetic energy suitable for injection into the ion trap. The ion volume and the first two elements of the source lens were electrically isolated and each could be held at any desired potential. The final element of the source lens was in electrical contact with the first element of the ion injection einzel lens, which was grounded. The second (central) element of the einzel lens was electrically isolated using sapphire balls, and could be held at any desired potential. The final element of the einzel lens was in electrical contact with the ion trap entrance electrode, and was held at ground potential during the period that the ions are admitted into the ion trap and at a voltage appropriate to the particular ion trap scan function otherwise.

The lenses of the Cs^+ gun were controlled with a custom designed power supply to permit the pulsing of the cesium beam under the control of the ion trap's single-board computer and data system. The Cs^+ extraction lens was switched from a positive potential, relative to the Cs^+ ion source, to a negative potential in order to focus the Cs^+ ions onto the probe tip during the ion injection phase of the experiment. The potentials applied to the elements of the Cs^+ gun were derived from a single common line, held at a potential of 5–7 kV with respect to earth ground. The Cs^+ source was held at the common potential and the Cs^+ gun exit lens was held at a variable voltage (typically -600 V) with respect to this. The Cs^+ extraction lens was held at -375 V when Cs^+ ions were to be emitted from the source, and at $+75$ V with respect to the common potential when no Cs^+ ions were to be emitted. Table 2 gives typical operating potentials for obtaining Cs^+ SIMS spectra.

The gating process was controlled by a TTL signal through an optical isolator capable of 20 kV isolation. This gate pulse was controlled with the 5 V TTL signal normally used to control the gate to the electron ionization source. The Cs^+ beam was typically on for between 20 and 50 ms.

CsI was used as the sample because of its characteristic ability to form regularly spaced cluster ions at very high masses. Primary Cs^+ ions desorbed

TABLE 2

Typical operating parameters for Cs^+ SIMS ionization

Cs^+ source	7 kV	Probe tip/ion volume	+4 to 10 V
Cs^+ extraction ON	−375 V[a]	Source lens 1	+1 V
Cs^+ extraction OFF	+75 V[a]	Source lens 2	0 V
		Source lens 3	0 V
		1st einzel lens	0 V
Cs^+ exit lens	−600 V[a]	2nd einzel lens	−18 V
Cs^+ current	2.1 mA	Helium pressure	1.3 mTorr

[a] Relative to the Cs^+ source potential.

$(CsI)_nCs^+$ (where $n = 1, 2, 3, \ldots$) cluster ions from a CsI sample on a stainless steel probe tip located outside of the ion trap assembly. The sample, dissolved in water, was applied to the probe and the solvent was evaporated in vacuo. The externally generated cluster ions are subsequently injected into the ion trap, where collisions with a high background pressure of helium (approximately 1 mTorr) allowed the ions to be trapped.

The peptide samples were prepared by adding 1 μl of a solution of peptide dissolved in 50:50 methanol/water solution to 1 μl of 1:1 thioglycerol/glycerol. The sample and matrix were mixed directly on the probe. The peptide samples were bombarded with 7 keV Cs^+ projectiles using a primary ion current of approximately 0.8 nA. An area of approximately 0.8 mm^2 of the probe was irradiated by the Cs^+ beam. The sputtered sample ions were injected into the ion trap at an r.f. potential corresponding to maximum ion trapping efficiencies. The relationship between injection efficiency and ion trap operating parameters is discussed elsewhere [20].

RESULTS AND DISCUSSION

Reduced size electrodes

Earlier studies showed that a two-fold reduction in the size of the ion trap electrodes could be used to obtain good quality EI mass spectra of fluorinated organics to the theoretical limit of approximately 2500 Da per charge [8]. In these studies, the high mass samples were ionized within the trapping volume of the ion trap by electron impact.

Desorption ionization and ion injection, previously performed on a full size ion trap [3] were implemented on the reduced scale devices. Figure 4a shows the mass spectrum of $(CsI)_nCs^+$ using the half-sized ion trap, where n denotes the cluster size. The complete sequence of CsI clusters is observed and that at m/z 2473, due to $C_{10}I_9^+$, is near the theoretical limit of the device.

Note the high performance over the entire mass-to-charge range. Resolution is approximately 1500 ($m/\Delta m$, where Δm is FWHM) at 2500 Da. Note,

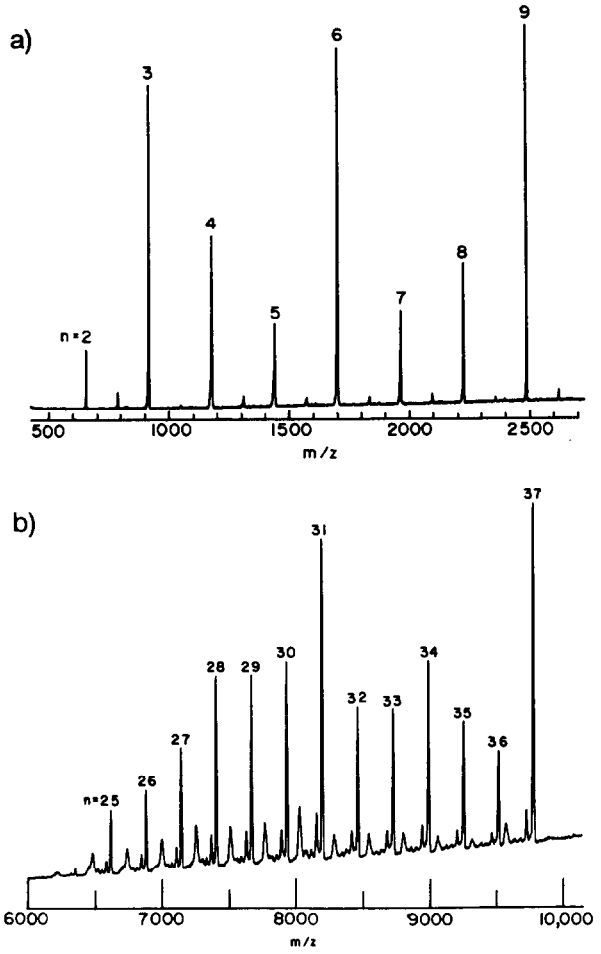

Fig. 4. Mass spectrum of $(CsI)_nCs^+$ obtained using Cs^+ SIMS ionization and ion injection into (a) the half-sized ion trap ($r_0 = 5$ mm); (b) the quarter-sized ion trap ($r_0 = 2.5$ mm).

however, that artifact signals of low intensity occur. It is believed that these are due to ions ejected prematurely because of imperfections in the r.f. field caused by the relatively large holes (1/16 in. diameter) in the end-cap electrodes. Measures to reduce these field imperfections were not attempted.

The half-sized electrodes were replaced with the quarter-sized electrodes (theoretical mass/charge limit = 10.4 kDa per charge) and CsI clusters re-analyzed. Figure 4b illustrates the mass spectrum in the range 6–10 kDa. Note again the high ion abundances out to the mass limit and the presence of artifact peaks among the sequence of cluster ions. Since the electrodes are smaller, the field faults (due to the apertures in the end caps) are more pronounced, leading to more intense artifacts than for the half-sized trap. The

resolution was measured to be approximately 1900 for $Cs_{38}I_{37}^+$ at m/z 9753. It is postulated that improvements in the quality of the trapping fields would lead to enhanced resolution. (Note that the peak widths increase with m/z in all the experiments described in this paper but not enough to offset the increase in resolution, $m/\Delta m$, as m increases.)

A reduction in the r.f. voltage ramp rate to produce a reduction in the m/z scan rate should further improve spectral resolution. The r.f. ramp rate the commercial system provides for a m/z scan rate is 180 μs per Da per unit charge. Upon increasing the mass range by a factor of four (half-sized electrodes) or sixteen (quarter-sized electrodes) by reducing the size of the electrodes, the m/z scan rates become 45 $\mu s\,Da^{-1}$ and 11 $\mu s\,Da^{-1}$, respectively. These scan rates have been found to be too fast for obtaining the best spectral resolution. Upon reducing the m/z scan rate to the normal 180 $\mu s\,Da^{-1}$ by simply altering the instrument software by introduction of an additional time delay after every r.f. DAC step during the mass analysis r.f. ramp, the resolution obtained using the quarter-sized trap could be enhanced by approximately a factor of two over what could be obtained with the initial faster m/z scan rates. The effect of scan rate on resolution is described in more detail in a later section of the paper.

Frequency reduction

As noted in Eq. (5), the mass limit of the ion trap, operated in the mass-selective instability mode, is inversely proportional to the square of the drive frequency. A reduction in this frequency below 1.1 MHz is therefore a second method to increase the mass range of the system above the commercial limit of 650 Da per charge. In this work, reductions in frequency to 0.92 MHz and then to 0.60 MHz were achieved. A comparison of the performance of the system operated at 0.60 MHz will be made relative to normal operation at 1.1 MHz. Note that frequency reduction was accompanied by changes in the r.f. amplitude so the theoretical mass limits are not simply predicted by the square of the change in frequency (see Experimental section).

Figure 5 illustrates the mass spectrum of RbI desorbed with 7 kV Cs^+ projectiles, recorded at a reduced drive frequency of 0.6 MHz. The observed mass limit is approximately 2050 Da (3.15 × increase). As indicated in this mass spectrum, the RbI ions form stable cluster ions much like CsI. Another interesting observation is the formation of ion/molecule products with Cs derived from the primary Cs^+ beam. Ions having structures corresponding to $(RbI)_nCs^+$, where $n = 2, 3, 5, 7$ are observed. The rate of the r.f. mass analysis scan in this mass spectrum is 60 $\mu s\,Da^{-1}$ and the resolution is approximately 450 at m/z 933 ($Rb_5I_4^+$) and twice this at m/z 1781 ($Rb_9I_8^+$). The resolution was increased to 900 and 1800, respectively, when the scan rate was reduced to 130 $\mu s\,Da^{-1}$. The scan rates were again reduced by introducing a variable

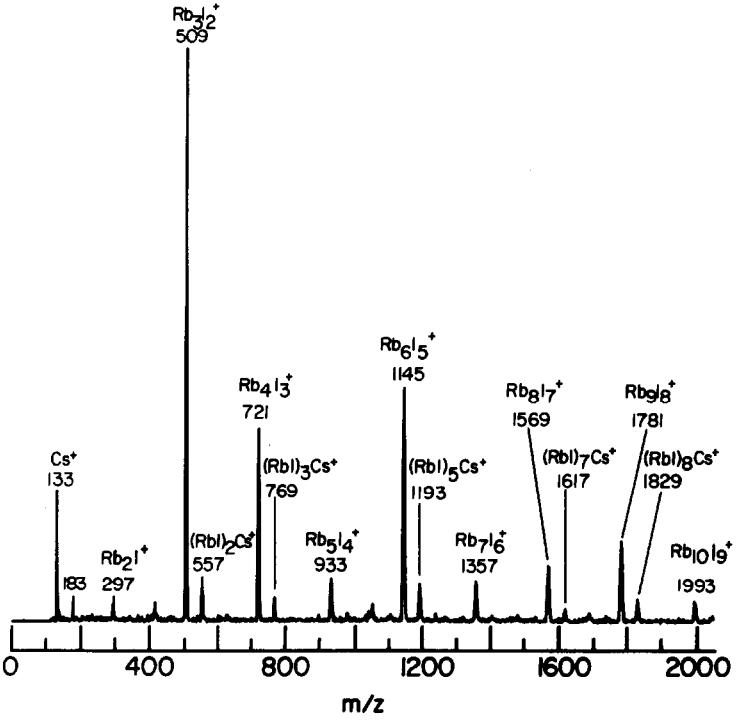

Fig. 5. Mass spectrum of RbI, obtained using Cs^+ SIMS ionization and ion injection. The r.f. drive frequency of the ion trap was reduced from 1.1 MHz to 0.6 MHz. The commercial set of electrodes (r_0 = 1 cm) was used.

delay (by modification of the ITMS software) after every DAC step of the mass analysis r.f. scan. Figure 6 illustrates the resolution enhancement achieved for two RbI clusters (Rb_2I^+, m/z 297 and $Rb_5I_4^+$, m/z 933) as the scan rate was decreased from 60 to 90 and then to 130 $\mu s\,Da^{-1}$. By reducing the scan rate in this way, it was not possible to baseline resolve the Rb^+ isotopes, which are separated by 2 Da. Slowing the scan rate below 130 $\mu s\,Da^{-1}$ by this method did not further improve the resolution.

To further explore the performance of the ion trap at 0.6 MHz, a CsI mass spectrum was obtained as shown in Fig. 7. A scan rate of 130 $\mu s\,Da^{-1}$ was used to achieve similar resolution to that obtained with RbI. Resolutions of 450 and 850 for CsI clusters at m/z 912 and m/z 1692, respectively, were recorded.

These data demonstrate that it is possible to extend the mass limit (as predicted from Eq. 5) as expected when the r.f. drive frequency of the ion trap is reduced. The data also indicate that resolution decreases at significantly lower drive frequencies even if the r.f. ramp rate is slowed to provide a m/z scan rate comparable to that of the standard system. However a relatively modest reduction in r.f. drive frequency shows no perceptible degradation in

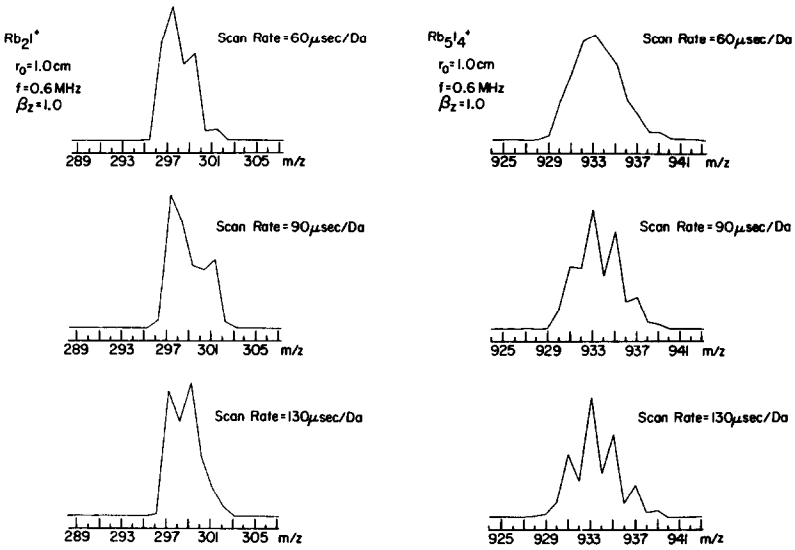

Fig. 6. Resolution enhancement of RbI isotopes (m/z 297 and 933) at reduced scan rates when the ion trap was operated at a drive frequency of 0.6 MHz.

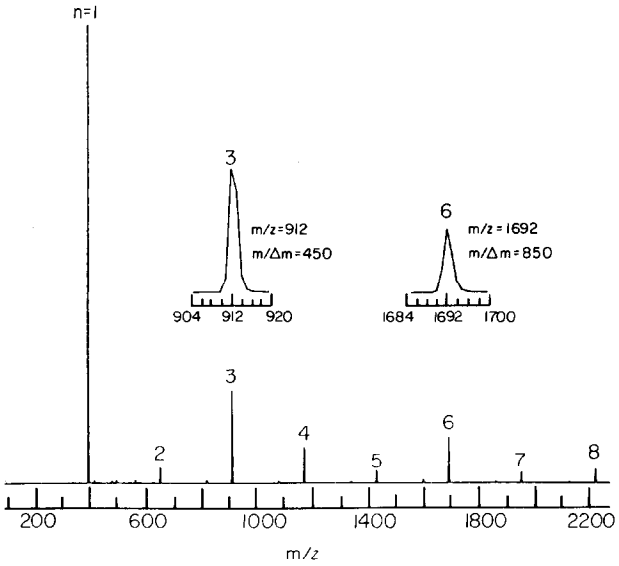

Fig. 7. Mass spectrum of CsI, obtained using Cs^+ SIMS ionization, ion injection, and a reduced scan rate of 130 $\mu s\,Da^{-1}$. The inserts show the resolution.

resolution. An insufficient number of drive frequencies were examined in order to completely characterize the frequency reduction at which loss of resolution becomes significant. Results described below (see the section on the

r.f. offset DAC) suggest that the observed resolution degradation may be in part due to the method used to reduce the r.f. ramp rate. Further characterization of the effect of drive frequency on resolution is clearly warranted and such work will be pursued.

Resonance ejection

The final method for mass range extension evaluated in this paper employs mass-selective instability but uses a novel technique for obtaining high mass information. Whereas the other methods require physical modifications to the ion trap or the system electronics, this method employs the simple expedient of applying an a.c. voltage of frequency less than one half of the drive frequency between the end-cap electrodes during the mass analysis scan. As such, it is related to the axial modulation experiments [21] used to excited ions for MS–MS in the ion trap and is referred to in the patent literature [22]. The earliest experimental work involving axial modulation [21] employed a frequency close to half the r.f. drive frequency (i.e. β_z is close to 1) and q_z was scanned while ejected ions were detected as usual with an external electron multiplier. It provided enhanced resolution but it was not used for mass range extension, being applied only in the special case where the a.c. voltage was nearly one-half the fundamental trapping frequency to increase the sensitivity of the system. Spectral peaks which were broadened to a width of about five mass units by space charge could be reduced in width to about one mass unit with this technique.

The mass-selective instability with resonance ejection method, referred to herein as either resonance ejection or as axial modulation, like the better known methods for performing MS–MS experiments [7], utilizes the long established method of resonance excitation. The difference between the resonance ejection method and resonant excitation as applied in tandem experiments is in the timing and, secondarily, in the intensity of the applied supplementary a.c. field. In tandem experiments, the supplementary a.c. voltage amplitude is typically below $3\,V_{p-p}$ and is applied prior to mass analysis when the r.f. voltage is fixed at a chosen level. If the amplitude of the supplementary a.c. voltage is significantly above this level, the excited ions are ejected from the ion trap before dissociation. In the resonance ejection experiments performed in this study, the supplementary a.c. voltage is applied during the r.f. scan with an amplitude typically $15\,V_{p-p}$ so that ions, when brought into resonance with the supplementary field, are excited to such an extent that they are ejected from the ion trap.

The effect of the applied a.c. supplementary field on the stability diagram can be visualized as producing a line of instability within the stable region corresponding to an iso-β_z line. The intersection of this line of instability with

the instrument scan line, which in the case of r.f.-only operation is the q_z axis, determines the q_{eject} value.

The factor by which the mass range is to be extended when using resonance ejection defines the value of q_{eject} and therefore the corresponding β_z value at which a resonance instability must be generated. This is because mass is linearly proportional to q_z and not β_z (see Eq. 3). The q_{eject} value necessary for a desired mass range extension, $m/z_{\text{limit-new}}$, can be calculated from the following proportionality obtained by rearranging Eq. (10) and cancelling terms.

$$q_{\text{eject-new}} = q_{\text{eject-old}}(m/z_{\text{limit-old}})/(m/z_{\text{limit-new}}) \tag{12}$$

For r.f. only operation at the standard drive frequency of 1.1 MHz, $q_{\text{eject-old}}$ and $m/z_{\text{limit-old}}$ represent the q_z at the stability limit, ca. 0.908, and the standard mass range, 650 Da, respectively. The relationship between q_z and β_z, shown for the r.f.-only case in Fig. 8, cannot be expressed in closed form. However, numerical procedures to accurately calculate β_{eject} from q_{eject} are relatively straightforward [15]. For cases where q_z is less than 0.4 and the system is operated r.f.-only, the approximate relationship

$$\beta_z = q_z/2^{1/2} \tag{13}$$

can be used. If, as in these experiments, only the first series of ion characteristic frequencies are to be used for resonance excitation, the appropriate frequency of the applied supplementary voltage, f_s, can be obtained from Eq. (14) once the required β_z has been established.

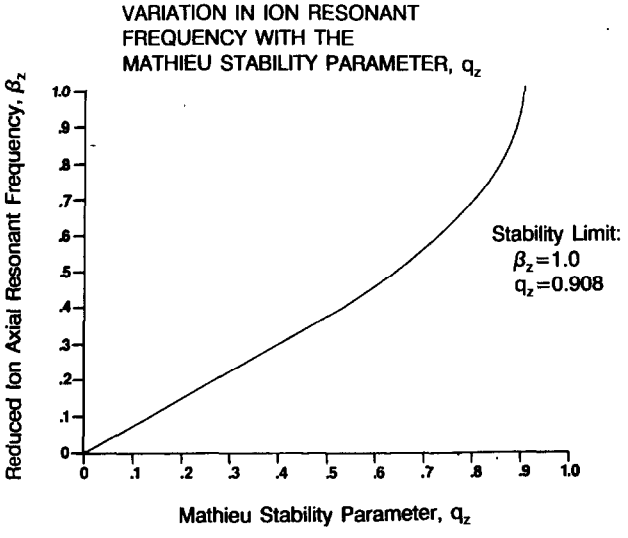

Fig. 8. Accurate relationship between the ion resonant frequency β_z to the Mathieu stability parameter q_z. (Courtesy J.N. Louris, Finnigan MAT.)

$$f_s = \beta_z f/2 \tag{14}$$

In this equation f denotes the r.f. drive frequency.

The mass range extension factor is calculated from the linear relationship between the point where the ion is to be ejected (q_{eject}) and the normal instability limit of $q_z = 0.908$. For example, to extend the mass range of the trap a factor of five above the normal 650 Da per charge range, the q_{eject} value should be 0.182 ($q_{eject} = 0.908/5$). From Eq. (13), the appropriate β_{eject} value and the frequency (Eq. 12) can be calculated for ions to be resonantly ejected from the ion trap so as to obtain a five-fold increase in mass range. In this example, the β_{eject} value is calculated to be 0.127 which corresponds to a frequency of 70 kHz, and this frequency is applied to the end-cap electrodes during the r.f. mass analysis scan to give the desired increase in mass per charge range.

It would seem that, in principle, the mass range of an ion trap can be extended indefinitely by choosing an appropriately low β_{eject}. Figure 9 shows how the mass range of an r.f.-only ion trap increases as β_{eject} is reduced. In practice, as will be discussed below, it has been possible to extend the mass range of an ion trap by about a factor of 60. Further mass range extension was precluded due to limitations of the electronics which generate the supplementary a.c. voltage rather than by any fundamental limitation of the technique.

In an attempt to determine the ultimate mass limit of the unmodified commercial ion trap, experiments were done on cluster ions generated by bombarding solid CsI with 7 keV Cs^+ ions. The continuous dynode electron multiplier was fitted with a 20 kV conversion dynode for these experiments in

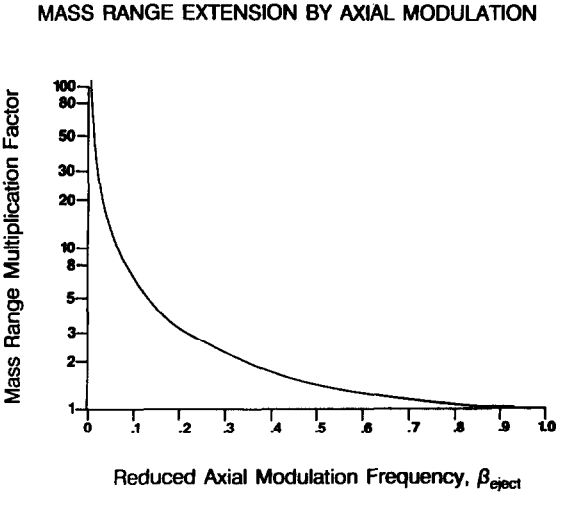

Fig. 9. Illustration of how the mass range is increased using axial modulation as one decreases the β_z of ejection. (Courtesy J.N. Louris, Finnigan MAT.)

order to improve sensitivity at high mass. The axial modulation frequency was reduced systematically, the lowest value used being 4600 Hz. When the applied frequency is 35.2 kHz, ejection occurs at q_z 0.091, which corresponds to $\beta_z = 0.064$ and $(m/z)_{max} = 6500$. These axial modulation conditions result in a mass limit which is ten-fold higher than the commercial system. Figure 10 illustrates the mass spectrum of the CsI clusters to $n = 22$. The maximum resolution which could be obtained by maintaining the normal scan rate of 180 μs Da^{-1} while enhancing the m/z range an order of magnitude was approximately 3000 at m/z 3500.

Figure 10 illustrates the characteristic features of the alkali halide ion abundance distributions, including the abundance of the $n = 13$ species which is greater than that of the $n = 12$ species, and the $n = 14$ and 15 species which are absent or of dramatically decreased abundance relative to the $n = 13$ and 16 ions. The latter characteristic repeats itself at $n = 22$–24. These features in the secondary ion mass spectra, which have been observed in less pronounced form previously [22], have led to postulations that the ion abundance enhancements (stable cluster ions) at the "magic numbers" $n = 13$, 22, 37 and 62 are due to stable "cubic-like" atomic arrangements of $3 \times 3 \times 3$, $3 \times 3 \times 5$, $3 \times 5 \times 5$ and $5 \times 5 \times 5$, where the numbers refer to the number of atomic species which define the cluster. The negative abundance deviations (i.e. $n = 14$ and 15) are thought to be due to the preferential unimolecular decay of the larger clusters to the more stable clusters. The distribution obtained

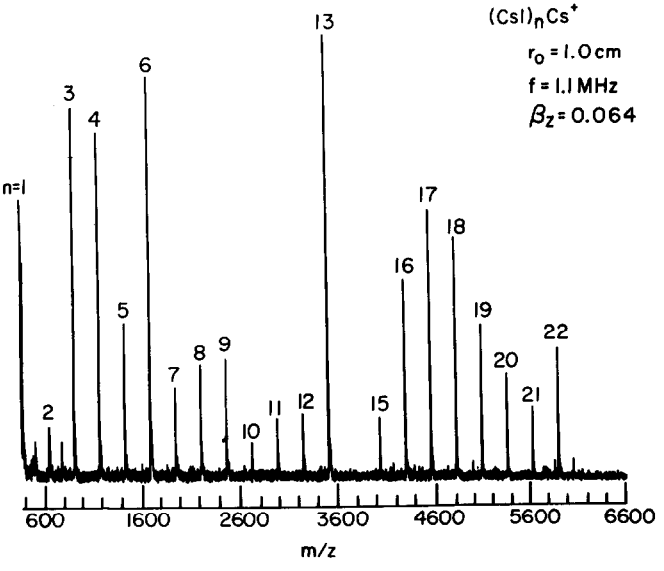

Fig. 10. Mass spectrum of CsI clusters acquired using an axial modulation frequency of 35.2 kHz ($q_{eject} = 0.0904$, $\beta_z = 0.064$). Cluster sizes of $(CsI)_nCs^+$ are indicated by values of n.

with a time-of-flight SIMS instrument when the ions were measured $< 1\,\mu s$ after emission showed no ion abundance anomalies [24]. This demonstrates that during the ion formation process, the cluster ions are not initially formed in their most stable configuration, but are emitted instead as metastable cluster ions which undergo unimolecular dissociations to form more energetically favored structures [25]. The ion trap, which operates on the millisecond time scale, enhances the kinetic effects which lead to intense "magic-number" ions.

In an attempt to achieve higher mass-to-charge ratios, resonance ejection was combined with reduction in the frequency of the ion trap which was reduced from 1.1 MHz to 0.92 MHz, thereby giving a 1.7-fold increase in mass. An axial modulation frequency of 4600 Hz ($\beta_z = 0.01$) was then applied to the end caps, giving an expected mass limit of approximately 72 000 Da (111-fold increase in mass). Figure 11 illustrates a region of the CsI mass spectrum from 22 to 46 kDa. The base peak, $(CsI)_{122}Cs^+$ ($n = 122$), m/z 31 830 corresponds to the stable $5 \times 7 \times 7$ cluster ion while m/z 44 560 corresponds to the $(CsI)_{171}Cs^+$ cluster and to a $3 \times 3 \times 19$ array.

Comparison of mass range extension techniques

The purpose of examining several methods for extending the mass range of the ion trap was to determine which method or combination of methods

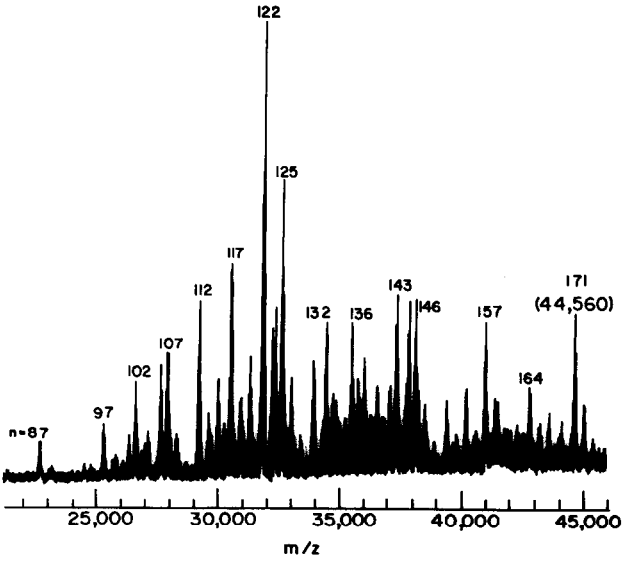

Fig. 11. Mass spectrum of CsI acquired using an axial modulation frequency of 4600 Hz ($q_{eject} = 0.02$, $\beta_z = 0.014$). The drive frequency was reduced from 1.1 MHz to 0.92 MHz to achieve an additional 1.7-fold increase in mass. Cluster sizes are indicated as in Fig. 10.

would result in the best performance at high mass. Used independently, resonance ejection has been shown to be the most successful method for analyzing extremely high mass ions; however, resolution, sensitivity and ease of operation are other factors which must be taken into account. Two separate comparisons were made: (i) using reduced radius electrodes relative to using resonance ejection for mass range extension, and (ii) using reduced drive frequencies relative to using resonance ejection for mass range extension.

An experiment was designed to compare the performance of the ion trap when operated under resonance ejection to the use of a reduced radius, both at a slightly reduced r.f. frequency (0.92 MHz). Operation at this lower frequency had no detrimental effect on the performance of the ion trap in either of the two mass extension modes. The injection conditions, mass limits and mass analysis scan rates were identical in the mass spectra taken in both experiments. Figure 12 compares the mass spectrum of CsI taken using

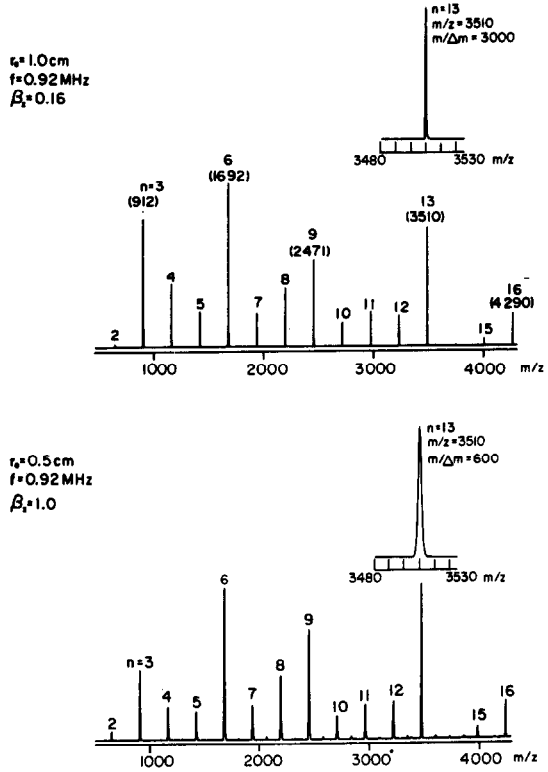

Fig. 12. Comparison of Cs^+ desorbed CsI spectra obtained from two different methods of extending the mass range of the ion trap. The mass range in the upper spectrum is increased by using resonance ejection whereas the lower spectrum shows mass range extension by halving the radius of the commercial electrodes. The conditions for trapping and the mass limit are identical in both spectra. The insert show the obtainable resolution of m/z 3510 with both techniques.

resonance ejection ($\beta_{eject} = 0.16$, $q_{eject} = 0.13$) conditions (upper spectrum) to that obtained when using the half-sized ion trap electrodes (lower spectrum). The mass/charge ratio limit in both experiments was 4420 Da per charge.

From this comparison, it is obvious that the mass spectra show excellent agreement although anomalous peaks thought to be due to field imperfections are present in the lower spectrum. The obtainable resolution is compared in the inserts, where $n = 13$ is shown in expanded form. As seen, the resolution is a factor of 5 higher when resonance ejection is the method chosen for mass range extension. However, when axial modulation was used at a frequency of 442 kHz ($\beta_z = 0.96$) with the half-sized electrodes, the resolution improved significantly, almost matching that obtained when the full-sized electrodes were used.

The same type of experiment was performed to compare resonance ejection on the full-sized system with the quarter-sized ion trap operating at the same reduced frequency, as shown in Fig. 13. The two spectra do not compare quite as well as when the half-sized ion trap was used and the anomalous peaks are

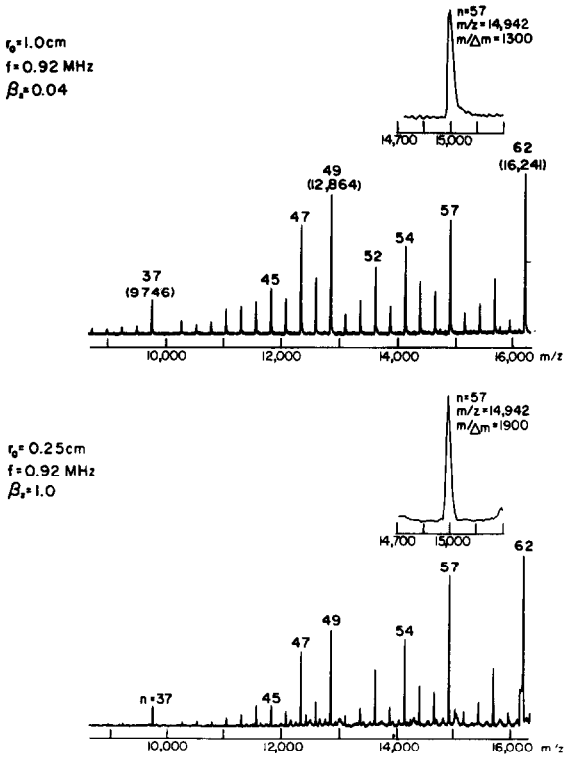

Fig. 13. Comparison of the CsI spectra obtained by using resonance ejection (upper spectrum) and by using quarter-sized ion trap electrodes. The inserts show the obtainable resolution at m/z 14942 with both techniques.

more pronounced. The inserts compare the resolution of the two techniques. In this case, resolution is slightly better with the quarter-sized electrodes compared to resonance ejection using the full-size system.

A comparison was also made between the mass spectrum of CsI obtained at a reduced drive frequency of 0.6 MHz (mass range = 2275 Da, 3.5 × extension) and the mass spectrum obtained using resonance ejection. Figure 14 shows this comparison where the upper spectrum is obtained at reduced frequency and the lower spectrum is obtained using axial modulation at a drive frequency of 1.1 MHz. The axial modulation frequency in the resonance ejection spectrum (104.5 kHz, or $\beta_z = 0.19$) was chosen to result in a mass limit identical to the reduced frequency spectrum. The r.f. level applied to the ring electrode during the injection period and the mass analysis r.f. scan rate are the same for both spectra. As observed in Fig. 14, the spectra are very similar; however, the inserts show that the resolution of the reduced frequency spectrum is approximately half that of the resonance ejection spectrum.

This comparison of obtainable resolution is even better illustrated in Fig. 15. This figure shows how well the two mass range extension methods are able to resolve the isotopes (2 Da apart) of two different RbI clusters at m/z 297 and m/z 933. Again, the upper part of this figure was obtained at a reduced frequency of 0.6 MHz, whereas the lower part of the figure was obtained using resonance ejection for mass range extension. The injection conditions and the

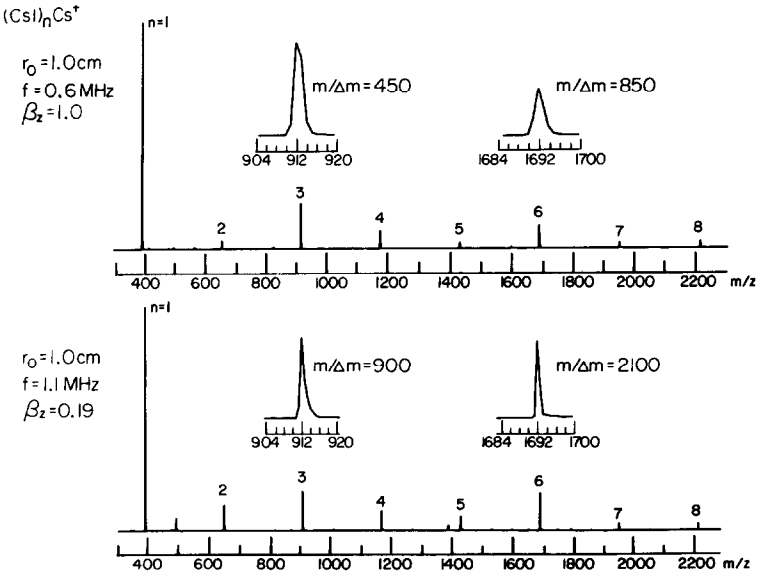

Fig. 14. Comparison of CsI spectra obtained by reducing the r.f. drive frequency (upper spectrum) from 1.1 MHz to 0.6 MHz and by extending the mass range using resonance ejection. The inserts illustrate the obtainable resolution for two different CsI clusters.

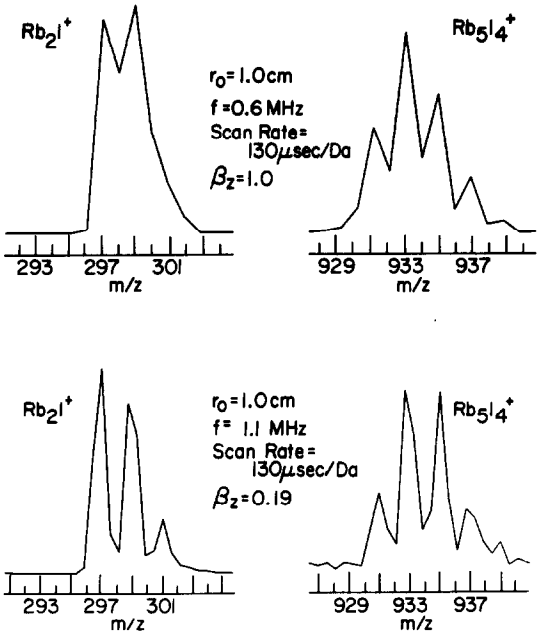

Fig. 15. Comparison of the obtainable resolution of two different RbI clusters at a drive frequency of 0.6 MHz and when using resonance ejection for mass range extension. The injection conditions were identical to those used in Fig. 14.

mass analysis scan rate are identical to those used for Fig. 14. As observed, the isotopes cannot be baseline resolved at reduced frequency while this is possible using axial modulation.

A reduction in the radius of the ion trap allows operation at higher mass than the commercial system. As a single mass range extension method, size reduction allows at least a 16-fold increase in mass. As shown above, the performance of the particular reduced radius systems available to us was inferior to the use of resonance ejection with the commercial set of electrodes. Extension of the mass range by a combination of size reduction with resonance ejection was therefore explored. Note, however, that the selection of the end-cap electrode aperture sizes in the reduced radius system may be the most significant factor controlling performance.

A combination of resonance ejection with the reduced radius ion traps showed only limited success. When axial modulation was used with the half-sized ion trap, it was only possible to reduce the ejection β_z value to approximately $\beta_z = 0.85$, which would result in only a slight increase in the mass limit of the half-sized ion trap (though the resolution did improve significantly at these axial modulation frequencies). Below $\beta_z = 0.85$, it was impossible to resonantly eject ions for mass range extension. When axial

modulation was implemented with the quarter-sized ion trap, the mass range could not be increased at any axial modulation frequency or modulation voltage. This result is surprising and is being explored further.

Resonance ejection can be utilized successfully with full-sized electrodes at a slightly reduced drive frequency of 0.921 MHz. This combination resulted in an additional 1.7-fold increase in mass over that available when using resonance ejection at a drive frequency of 1.1 MHz. Using this combination as already noted, ions could be resonantly ejected at β_z values as low as $\beta_z = 0.01$ (axial modulation frequency = 4505 Hz), which corresponds to $(m/z)_{max}$ of over 71 000 Da per charge. As demonstrated earlier, a significant reduction in the drive frequency to 0.6 MHz showed inferior performance to the use of axial modulation at a drive frequency of 1.1 MHz. In the reduced frequency experiments, ions were ejected from the ion trap at the normal mass-selective instability limit of $q_z = 0.908$.

It is conceivable that application of an axial modulation frequency near $\beta_z = 1$ would better resolve ions and that resonant ejection of ions at further reduced β_z values would further increase the mass range of the commercial sized ion trap ($r_0 = 1$ cm). The following is a description of a set of experiments intended to demonstrate if such advantages could indeed be realized.

To test whether axial modulation could increase resolution when the drive frequency was 0.60 MHz, RbI was used as the sample to see how well the isotopes could be resolved. Figure 16 illustrates the results for two different

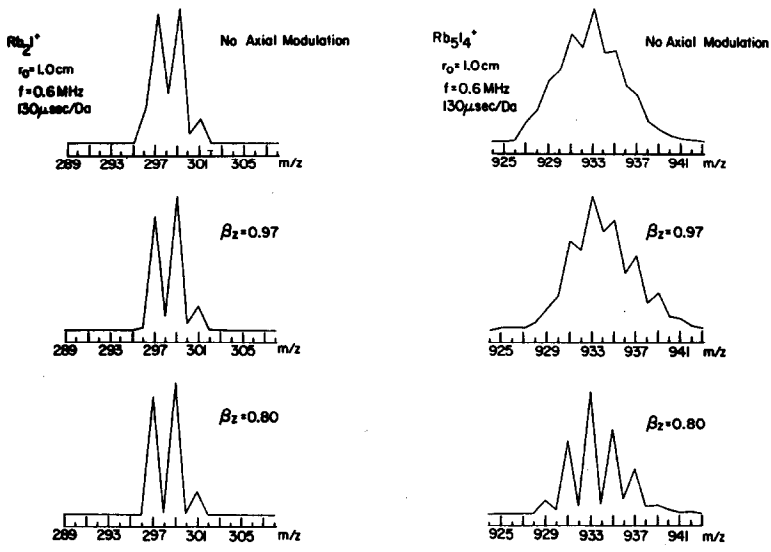

Fig. 16. The resolution for the isotopes of RbI clusters of m/z 297 and 933 are illustrated where no axial modulation was used (top spectra) and under conditions where axial modulation frequencies corresponding to $\beta_z = 0.97$ and $\beta_z = 0.8$ were used to increase performance.

RbI clusters at m/z 297 and m/z 933. The mass analysis scan was set to $130\,\mu s\,Da^{-1}$, which was found earlier to be a sufficient scan rate for efficient ion ejection. As shown in Fig. 16, operating with axial modulation at $\beta_z = 0.8$ (240 kHz applied across the end-cap electrodes) effectively increases the resolution of the system. The RbI clusters are resolved to baseline yielding resolutions better than that obtained when only resonance ejection is used at a drive frequency of 1.1 MHz, as demonstrated in Fig. 15. The resolution is approximately two times better when axial modulation is used with an r.f. drive frequency of 0.6 MHz than when axial modulation is not used. Attempts to produce a significant increase in mass range by using axial modulation in combination with a reduced drive frequency of 0.6 MHz showed only limited success. Resonant ejection occurred only when β_{eject} was greater than 0.7. The reason for this result has yet to be determined and will be the subject of further investigation.

Resolution enhancement using an offset r.f. DAC

In the work described above, the m/z scan rate was shown to be very important in determining the mass resolution of an ion trap when operated with an extended mass range. The observed mass resolution degraded at m/z scan rates appreciably greater than that of the commercial system, $180\,\mu s\,Da^{-1}$. (This may in part be due to the bandwidth of the electrometer used to amplify and convert the low level ion current signal into a high level voltage signal.) Furthermore there seemed to be no advantage in using slower m/z scan rates as no improvement in mass resolution was observed when this was attempted. However as, mentioned earlier, the method used to vary the m/z scan rate was to change the time period between the incremental changes in output of the 12-bit DAC controlling the r.f. voltage amplitude (DAC steps) when ramping the r.f. voltage during mass analysis. The entire procedure has a number of consequences that may have had a substantial effect on the experimental results.

When operating with the standard mass range and m/z scan rate, the time interval between DAC output increments is sufficiently short that the r.f. control system is unable to track individual DAC output steps. In this case the r.f. amplitude varies to a good approximation as a continuous ramp. When operating with an extended mass range with the time interval between r.f. DAC steps extended sufficiently to produce m/z scan rates in the range of $180\,\mu s\,u^{-1}$, the amplitude of the r.f. drive voltage tracks the "stair step" wave form output by the r.f. DAC. Furthermore, these steps are potentially quite coarse in terms of the incremental change of the mass at the threshold of instability with each step of the r.f. amplitude. For example, if the mass range is extended to 6500 Da, a ten-fold extension from the standard mass range, a

sudden 1.6 Da change occurs in the mass of ions at the threshold of instability per r.f. DAC output increment. This coarseness in the change in the mass at the threshold of instability per DAC output step scales proportionally with the degree of mass range extension no matter what method of mass range extension is used.

Significantly, the design of the commercial ion trap is such that the time interval between ADC samples of the ion current signal is always the same as the interval between r.f. DAC increments. Therefore, density of ADC samples per unit mass varies inversely with the factor by which the mass range is extended. The ADC sample density of the system, when operated with its standard mass range, is only 6.3 ADC samples per Da. When the mass range is extended beyond 4100 Da the sample density drops to less than one ADC sample per Da. Furthermore, information theory and experience dictate that it requires, as a minimum, about six samples across an entire mass peak in order to represent its peakshape with reasonable accuracy. This means that, without special modification, the instrument will have great difficulty in accurately representing any mass peaks which have a FWHM resolution in excess of about 1800 no matter what the mass range of the instrument. This correlates well with the upper limits of resolution observed in the previously described experiments.

In an attempt to circumvent these limitations without undertaking a complete redesign and replacement of the existing r.f. control and data acquisition system, an r.f. control scheme utilizing a supplementary DAC was implemented. The basic idea of the scheme was that if the scaling between the r.f. DAC output and the actual r.f. voltage amplitude applied to the ion trap ring electrode was reduced in inverse proportion to the factor by which the mass range of the instrument was being extended the number of DAC increments and ADC samples per mass unit (and per unit time) during the mass analysis r.f. voltage ramp would remain unchanged. Doing this alone would not solve the entire problem, as the mass range over which mass spectral data can be acquired would remain unchanged at 650 Da even though the intrinsic mass range of the instrument would be extended. This limitation was overcome by connecting the output of a supplementary DAC into the r.f. amplitude control circuitry so that the amplitude of the r.f. would respond proportionally to the scaled sum of the r.f. DAC and supplementary DAC outputs. This scheme allows the amplitude of the r.f. voltage applied to be the composite of a ramp controlled by the r.f. DAC and an offset controlled by the supplementary DAC. This enables the full mass range of the instrument to be accessed while maintaining appropriate r.f. DAC scaling and ADC sampling density. The limitation of this scheme is that only a 650 Da segment of the entire mass range may be scanned in any one experiment.

Since the planned extended mass range experiments did not require applica-

tion of d.c. voltages to ion the trap, the 16-bit DAC normally used to control the amplitude of the d.c. voltage applied to the ion trap was available for use as the supplementary or offset DAC. Using the d.c. DAC as the offset DAC was also advantageous since the d.c. DAC was already under the complete control of the instrument control software so no software had to be modified to perform the desired experiments. Figure 17 shows a simplified schematic of how the offset DAC scheme was implemented. The scaling between the r.f. DAC output (0–10 V), V_1, and the amplitude of the r.f. applied to the ring electrode, V_{RF}, was controlled by a variable resistor, R_1. The scaling between the offset DAC output (0–10 V), V_2, and V_{RF} was fixed so that when the output of the r.f. DAC was zero, full scale output of offset DAC corresponded to the maximum available r.f. voltage amplitude, $V_{RF\text{-}MAX}$.

Figure 18 illustrates the scan diagrams for resonance ejection in the situation when the trap is operated with a mass limit of 1950 Da, or three times the normal mass limit and compares this with the situation when the offset DAC scheme is not utilized. Under this latter condition, the r.f. DAC output is scaled to control the entire range of r.f. amplitude that can be applied to the ring electrode. During the mass analysis r.f. ramp, ions with masses from 30 to 1950 Da are ejected from the ion trap at a m/z scan rate of 60 μs Da^{-1} (one third of 180 μs Da^{-1}) which results in resolution degradation because of the relatively fast scan rate. When the offset DAC arrangement is used to keep the

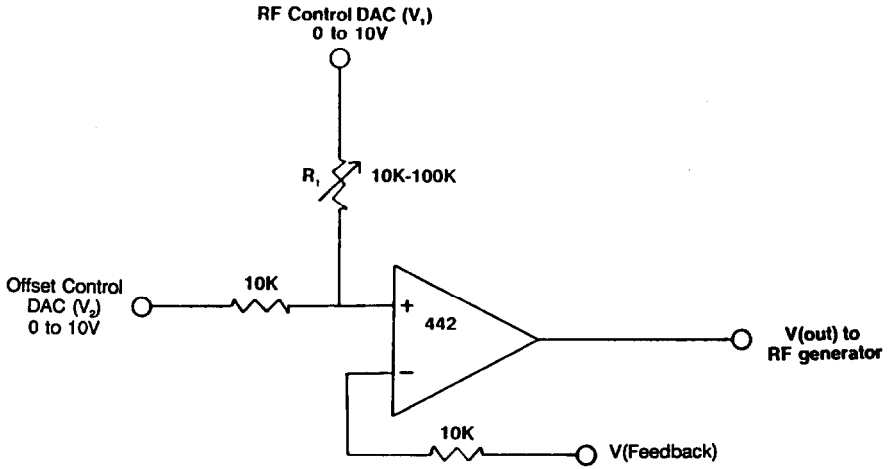

$$V_{RF} = V_{RF_{max}}\left(\frac{V_2}{10} + \frac{10K}{R_1}\cdot\frac{V_1}{10}\right)$$

Fig. 17. Circuit schematic illustrating the summing of the attenuated r.f. control 12-bit DAC with a 16-bit DAC (normally used to control the DC voltage applied to the ring electrode). This circuit allows for achieving a constant r.f. mass analysis scan rate over any mass range.

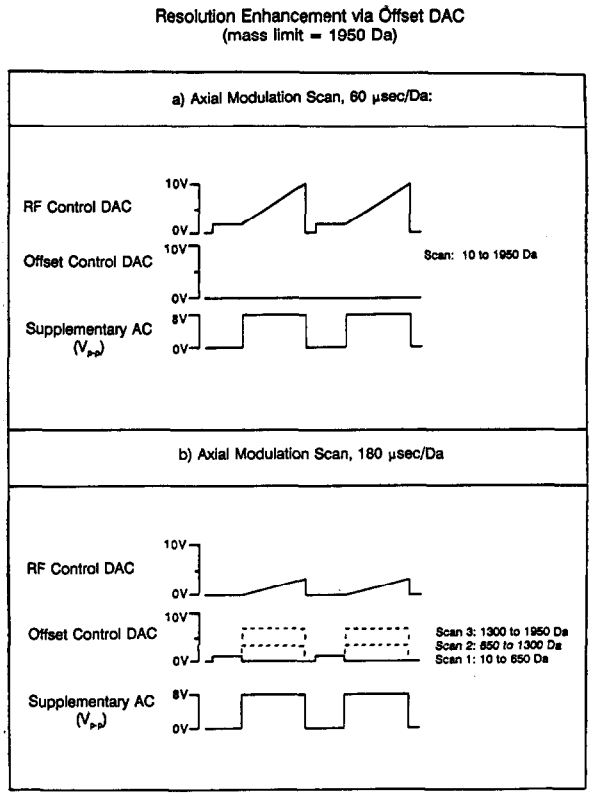

Fig. 18. Scan diagram illustrating how the scan rate of the r.f. mass analysis scan is controlled using the offset DAC method. (a) Fast scan conditions when the mass range is set to three times the normal mass limit using axial modulation. No DAC offset is used thereby resulting in a scan rate of $60\,\mu s\,Da^{-1}$. (b) Control of the scan rate via offsetting the r.f. DAC with a 16-bit DAC. The scan rate is kept constant at $180\,\mu s\,Da^{-1}$.

m/z scan rate constant at $180\,\mu s\,Da^{-1}$, the r.f. DAC output is scaled to control only a third of the entire range of the r.f. amplitude that can be applied to the ring electrode. The full mass spectrum is acquired in three segments: (1) the offset DAC is set to have zero output during the first stage of the scan covering the range between 30 Da and 650 Da, (2) the offset DAC is set to one third its full scale output while the range between 650 Da and 1300 Da is analyzed, and (3) the offset DAC is set to two thirds of its output and the range between 1300 Da and 1950 Da is analyzed.

The consequences of utilizing the offset DAC procedure are illustrated in Fig. 19 which is the $(M + H)^+$ region of the 15 amino acid peptide, Prepro VIP/PHM (m/z 1680). Cs^+ SIMS was used for ionization and the mass/charge limit for this experiment was set to 1950 Da per charge using axial modulation. The commercial set of electrodes ($r_0 = 1$ cm) at a normal drive frequency

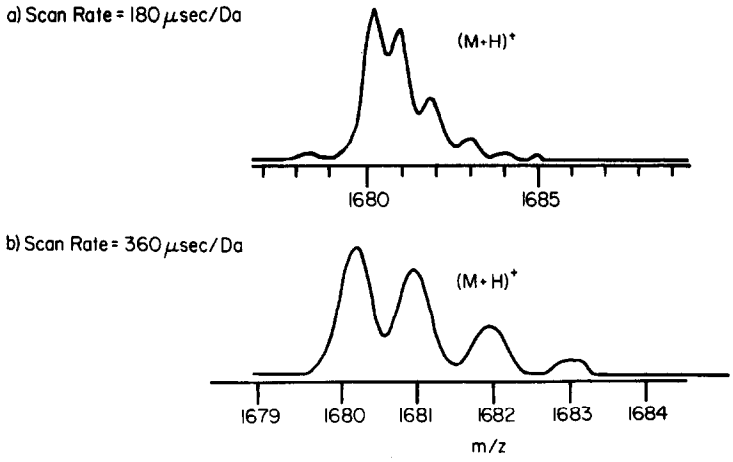

Fig. 19. Illustration of resolution enhancement using the offset DAC method for the $(M + H)^+$ ion of the peptide, Prepro VIP/PHM (MW = 1680).

of 1.1 MHz were used. As observed, the isotope peaks are well resolved with a calculated resolution of approximately 2500.

Figure 20 illustrates the resolution obtained at still higher mass/charge ratios for the isotopes of the cluster $Rb_{14}I_{13}^+$ in which the Rb isotopes are 2 Da apart. The mass limit of the system was increased to 3250 Da (5× mass increase) and the scan rate was set to 360 $\mu s\,Da^{-1}$ by attenuating the scaling between the r.f. DAC output and applied r.f. voltage amplitude by a factor of

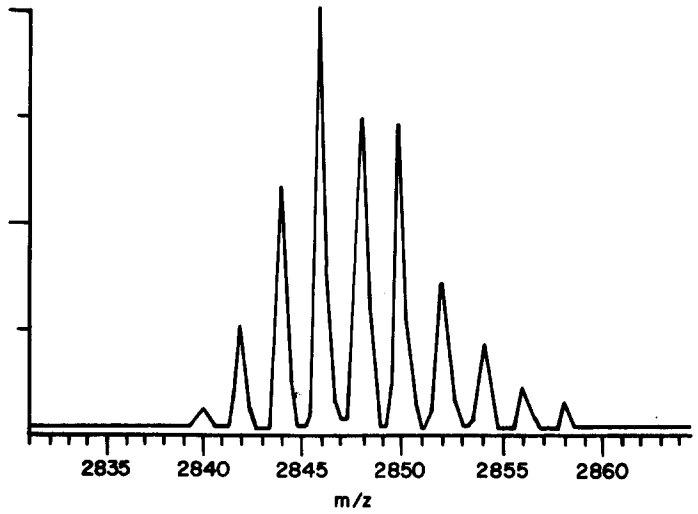

Fig. 20. Resolution enhancements of $Rb_{14}I_{13}^+$ (m/z 2846) using the offset DAC method at a scan rate of 360 $\mu s\,Da^{-1}$.

10. As observed, the isotope peaks are fully resolved and the resolution (FWHM) estimated to be 5000.

As seen from these results, the ion trap can be operated with close to unit resolution to approximately 3000 Da. As the mass range is further increased, a resolution of approximately 2000 is typically achieved when operated in the mass range of 6000 Da per charge. The offset DAC procedure allows slower scanning over the mass range and recovery of some of the resolution available in the experiment. Earlier studies showed similar enhancements when the scan rate was slowed by adding pauses between every DAC step; however, the resolution enhancement was not quite as good as shown with the offset DAC. This confirms that not the scan rate alone but control of the number of r.f. DAC increments and DAC steps taken over a particular mass range is of critical importance. The offset DAC procedure as implemented allows at least 6.3 bits of information to be taken for every m/z unit to a mass limit of 6500 Da per charge.

Mass measurement accuracy with resonance ejection

Resonance ejection has been determined to be the most easily implemented and the best single method for extending the mass range of the quadrupole ion trap. No changes to the physical nature of the ion trap electrodes or modifications to the commercial electronics are necessary.

However, when using axial modulation for mass range extension, a substantial mass shift, which depends upon the frequency and the amplitude of the supplementary voltage applied between the end-cap electrodes, is observed. In the early experiments with the axial modulation technique it was observed that as the amplitude of the supplementary voltage was increased, the mass peaks shifted to lower apparent masses. The amount of the mass shift was also observed to be mass dependent. The importance of characterizing this effect is immediately apparent as it affects mass calibration. The purpose of the experiments described in this section was to characterize and quantify the parameters that control this mass shift effect.

The mass shift due to resonance ejection was analyzed under two different axial modulation conditions: (1) $\beta_z = 0.129$ ($q_{\text{eject}} = 0.1816$, mass range = 3250 Da) and at (ii) $\beta_z = 0.0645$ ($q_{\text{eject}} = 0.0908$, mass range = 6500). Plots of the mass shift vs. axial modulation voltage amplitude were made for various cluster ions at the two different axial modulation frequencies. An example of this type of plot for $Cs_7I_6^+$ at m/z 1692 ($\beta_{\text{eject}} = 0.129$) is shown in Fig. 21. As the amplitude of the axial modulation voltage is increased, the shift in mass becomes more pronounced. This plot also suggests that there is a minimum amplitude at which the ions can be resonantly ejected from the ion trap. In this case, 4.5 V_{p-p} is necessary to eject m/z 1692 at $q_{\text{eject}} = 0.182$. Above a certain

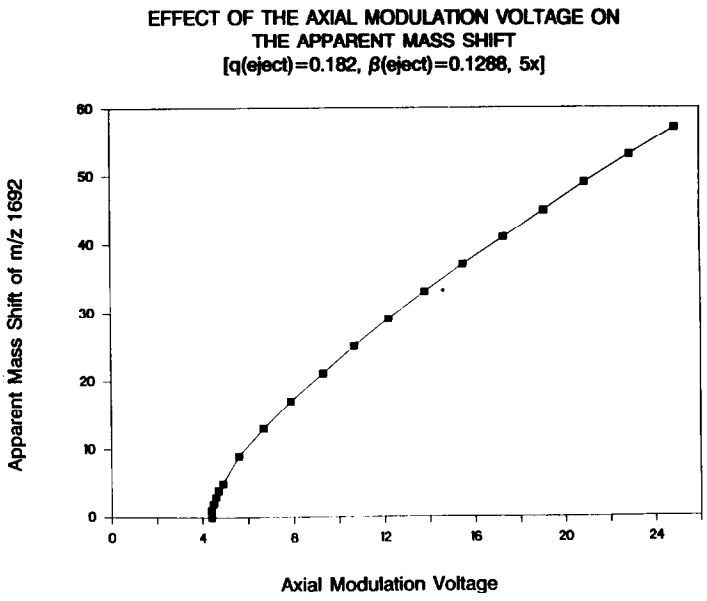

Fig. 21. Effect of axial modulation voltage on the apparent mass shift for m/z 1172 ($Cs_5I_4^+$) at $\beta_{eject} = 0.1288$.

threshold, the mass shift is linear with increasing axial modulation voltage. At lower mass, this type of plot reveals an even larger absolute mass shift, and alternatively a smaller apparent mass shift at higher masses.

In order to calibrate a mass spectrum, the apparent mass of an ion must be independent of the chosen mass range. From plots like Fig. 21, it is possible to determine a relation between the axial modulation voltage and mass shift. Figure 22 gives the results at $\beta_{eject} = 0.107$. As observed in this plot, a linear relationship is observed between the mass shift and the mass of the ion. In other words, it is necessary to ramp the axial modulation voltage linearly with the r.f. mass analysis scan in order to have a constant mass shift. This is a very important result for calibration of the system at high mass.

The mass shift for a particular ion is not only dependent on the axial modulation voltage but also, not surprisingly, on the modulation frequency i.e. on β_{eject}. Figure 23 shows this effect for ions of m/z 1172. The rate of increase of amplitude of the axial modulation voltage with r.f. voltage amplitude during mass analysis would have to be greater at high β_{eject} values in order to maintain a constant mass shift with mass. Note, however, that this requirement does not allow the magnitude of the axial modulation voltage to be simultaneously optimized for sensitivity which it also effects.

As described, a constant axial modulation voltage will shift the apparent mass of an ion. It is possible to scan the axial modulation voltage amplitude

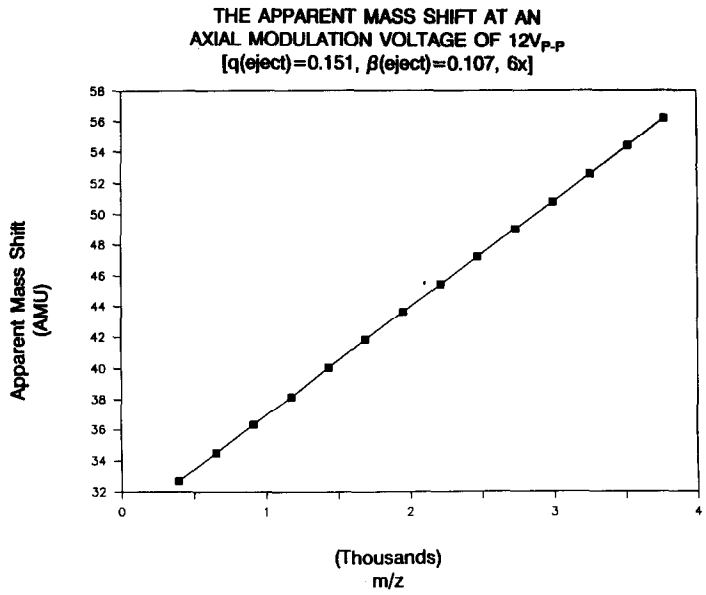

Fig. 22. The apparent mass shift for various CsI clusters at a constant amplitude of axial modulation of $12\,V_{p\text{-}p}$ when the mass range was extended by a factor of 6 ($q_{eject} = 0.151$, $\beta_{eject} = 0.107$).

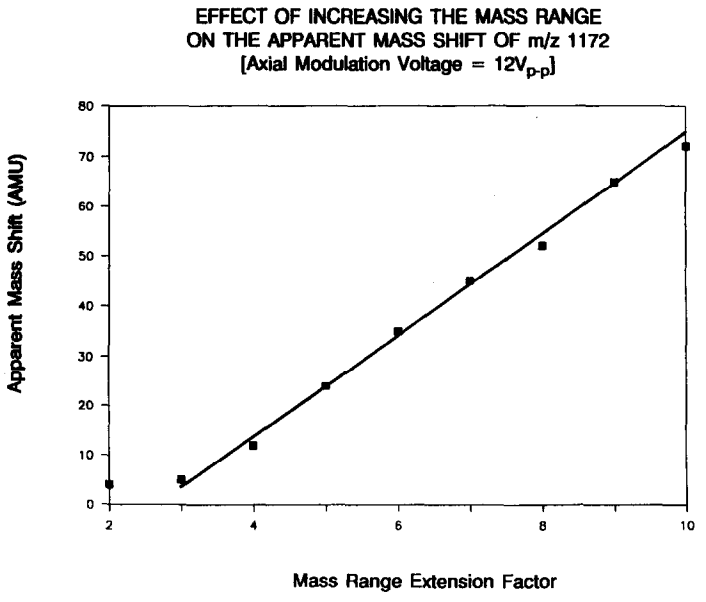

Fig. 23. Effect of increasing the mass range of the apparent mass shift of m/z 1172 ($Cs_5I_4^+$) at a constant axial modulation voltage.

to yield a constant apparent mass shift for calibration of the system, however, since the capability is not currently implemented for routine ion trap operation, it is desirable to be able to assign m/z values to ions in with a high degree of accuracy without scanning the axial modulation voltage. An experiment was therefore done on Prepro VIP/PHM, a 15 amino acid peptide having a molecular weight of 1680 Da, to test the ability to assign masses to a simulated "unknown" when using the CsI data as calibration plots. This peptide dissociates to give known sequence specific fragment ions, making it possible to use it to determine the mass assignment accuracy at high mass. The mass range was extended by factors ranging from two to five, using identical axial modulation conditions to those for the calibration plots. Mass spectra of Prepro VIP/PHM were obtained at the different mass range extension factors and apparent mass assignment were adjusted as dictated by the CsI calibration plots. Figure 24 shows the highest error associated with assigning the masses to the $(M + H)^+$ ion and the fragment ions at increasing mass range multiplication factors. For example, using the generated calibration plots, it was possible to determine the mass of the ions within zero to 1.5 Da from the actual mass when the mass range was extended by a factor of three. There appeared to be no systematic error in assigning the m/z values. The mass measurement accuracy was not tested beyond a mass range multiplication factor of five.

From this study, we have determined that it is possible to assign masses to better than 0.1% accuracy at extended mass ranges when a constant axial modulation voltage is used and a calibration curve is generated. Until a method is devised to insure that the mass range is linear with the r.f. voltage

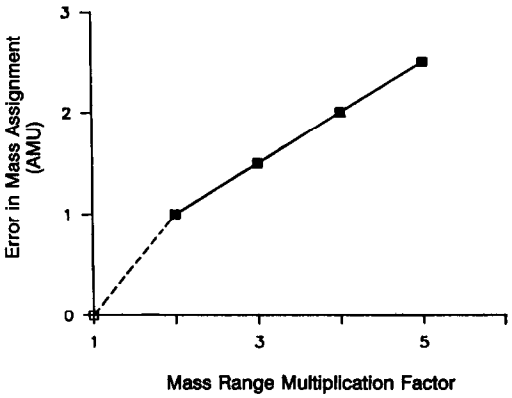

Fig. 24. Mass measurement accuracy when using resonance ejection with an external mass calibration routine. The filled data points are experimentally determined errors for the 15 amino acid peptide (KQLQQPFNPSQGQSS).

scan (i.e. by scanning the axial modulation voltage with the r.f. voltage), it will be necessary to utilize an external calibrant prior to running an unknown sample. CsI cannot be used as an internal calibrant for liquid SIMS experiments because desorption efficiencies are significantly decreased by its presence in the sample, although dual beam methods of internal calibration are conceivable.

CONCLUSIONS

Three methods have been used for extending the mass range of the quadrupole ion trap, operated in the mass-selective instability mode. Reduction in the trapping dimensions has resulted in a 16-fold increase in mass to 10.4 kDa, though field faults in these small electrodes resulted in poor resolution and observation of artifacts. Frequency reduction also extends the mass range, showing no noticeable decrease in performance at 0.92 MHz (1.7-fold increase in mass) but a significant loss of resolution on reduction in frequency to 0.6 MHz. Only two drive frequencies, 0.92 MHz and 0.6 MHz, were studied due to a limited availability of crystal oscillators. It is quite conceivable that a reduction in the drive frequency below 0.92 MHz would yield excellent results.

The most successful single method for mass range extension is mass-selective instability with resonance ejection. This axial modulation technique offers the best sensitivity together with the advantage that no instrumental nor physical modifications to the ITMS electronics or ion trap structure were required. By using a combination of resonance ejection and a reduced frequency, masses in excess of 70 000 Da per charge have been observed. A more significant reduction in frequency to 0.6 MHz, while still using resonance ejection, resulted in poorly ejected ions at β_z values below 0.8. It is conceivable that a modest reduction in frequency and using a slightly reduced radius ion trap with axial modulation may result in observation of ions to even higher masses with high performance.

The offset DAC procedure allows for easy control of the r.f. mass analysis scan rate as well as the number of r.f. DAC increments and ADC samples per unit mass scanned with the ion trap. This development has shown that unit mass resolution can be achieved for inorganic salts at mass/charge ratios approaching 3000 Da per charge.

The occurrence of systematic mass shifts in the axial modulation experiment has been characterized and related to the amplitude and frequency of the axial modulation voltage. The effects are easily corrected using an external standard and a first order correction yields mass measurement errors of no more than 0.1%, i.e. $\leqslant 3$ Da for organic compounds at m/z 3000.

ACKNOWLEDGMENTS

This work was supported by the National Science Foundation (CHE 87-21768). We also acknowledge support of the Purdue work by Finnigan MAT through the Industrial Associates Program.

REFERENCES

1 J.S. Brodbelt, J.N. Louris and R.G. Cooks, Anal. Chem., 59 (1987) 1278.
2 S.A. McLuckey, G.L. Glish and P.E. Kelley, Anal. Chem., 59 (1987) 1670.
3 J.N. Louris, J.W. Amy, T.Y. Ridley and R.G. Cooks, Int. J. Mass Spectrom. Ion Processes, 88 (1989) 97.
4 S.A. McLuckey, G.L. Glish and K.G. Asano, Anal. Chim. Acta, 225 (1989) 25.
5 R.E. Kaiser, Jr., J.N. Louris, J.W. Amy and R.G. Cooks, Rapid Commun. Mass Spectrom., 3 (1989) 225.
6 G.J. Van Berkel, G.L. Glish and S.A. McLuckey, Anal. Chem., 62 (1990) 1284.
7 J.N. Louris, R.G. Cooks, J.E.P. Syka, P.E. Kelley, G.C. Stafford, Jr. and J.F.J. Todd, Anal. Chem., 59 (1987) 1677.
8 R.E. Kaiser, Jr., R.G. Cooks, J. Moss and P.H. Hemberger, Rapid Commun. Mass Spectrom., 3 (1989) 50.
9 G.C. Stafford, Jr., P.E. Kelley, J.E.P. Syka, W.E. Reynolds and J.F.J. Todd, Int. J. Mass Spectrom. Ion Processes, 60 (1984) 85.
10 B.D. Nourse and R.G. Cooks, Anal. Chim. Acta, 228 (1990) 1.
11 R.E. March, R.J. Hughes and J.F.J. Todd, Quadrupole Storage Mass Spectrometry, Wiley, New York, 1989.
12 S.A. McLuckey, G.L. Glish, K.G. Asamo and G.J. Van Berkel, Anal. Chem., 60 (1988) 2312.
13 R.F. Bonner, G. Lawson, J.F.J. Todd and R.E. March, Adv. Mass Spectrom., 6 (1974) 377.
14 E. Fischer, Z. Phys., 156 (1959) 1.
15 W. Paul, H.P. Reinhard and V. von Zahn, Z. Phys., 152 (1958) 143.
16 R.D. Knight, Int. J. Mass Spectrom. Ion Phys., 51 (1983) 127.
17 G.C. Stafford, Jr. and J.E.P. Syka, unpublished results.
18 J.F.J. Todd, J.J. Bexon, M. Weber-Grabau, P.E. Kelley, G.C. Stafford, Jr. and R.D. Smith, Proc. 35th ASMS Conf. on Mass Spectrometry and Allied Topics, Denver, CO, 1987, p. 263.
19 W. Aberth, K.M. Straub and A.L. Burlingame, Anal. Chem., 54 (1982) 2029.
20 R.E. Kaiser, Jr. and R.G. Cooks, unpublished work.
21 M. Weber-Grabau, P.E. Kelley, S.C. Bradshaw and D.J. Hoekman, Proc. 36th ASMS Conf. on Mass Spectrometry and Allied Topics, San Francisco, CA, 1988, p. 1106.
22 J.E. Campana, R.M. Barlak, R.J. Colton, J.J. DeCorpo, J.R. Wyatt and B.I. Dunlap, Phys. Rev. Lett., 47 (1981) 1046.
23 T.M. Barlak, J.R. Wyatt, R.J. Colton, J.J. DeCorpo and J.E. Campana, J. Am. Chem. Soc., 104 (1982) 1212.
24 W. Ens, R. Beavis and K.G. Standing, Phys. Rev. Lett., 50 (1983) 27.
25 J.E. Campana and B.I. Dunlap, Int. J. Mass Spectrom. Ion Processes, 57 (1984) 103.